Research Square

Preprints are preliminary reports that have not undergone peer review.
They should not be considered conclusive, used to inform clinical practice,
or referenced by the media as validated information.

Quantifying Prematurity-Related Lung Disease in Adulthood using Magnetic Resonance Imaging (MRI) in adolescent sheep born premature: A pilot study

Tim Brokken
Maastricht University Medical Centre
Sophie M.L. Neuen
Maastricht University Medical Centre
Matthias C. Hütten
Maastricht University Medical Centre
Remco G.C. Santegoeds
Maastricht University Medical Centre
Daan Caudri
Erasmus MC - Sophia Children's Hospital
Pierluigi Ciet
Erasmus MC
Merlijn Bonte
Erasmus MC - Sophia Children's Hospital
Luc Zimmermann
Maastricht University Medical Centre
Daan R.M.G. Ophelders
Maastricht University Medical Centre
Niki L. Reynaert
Maastricht University Medical Centre
Tim G.A.M. Wolfs
Maastricht University Medical Centre
Sami O. Simons
sami.simons@mumc.nl
Maastricht University Medical Centre

Research Article

Keywords: Neonatal respiratory disease, ovine model, lung development, pulmonary imaging, long-term respiratory outcomes

Posted Date: November 5th, 2026

DOI: https://doi.org/10.21203/rs.3.rs-11433375/v1

License: This work is licensed under a Creative Commons Attribution 4.0 International License. Read Full License

Additional Declarations: Competing interest reported. SOS reports grants from Roche, Dutch Research Council (NWO) and Lung Foundation Netherlands (Longfonds); Honoraria for lectures from AstraZeneca,Chiesi, and Johnson & Johnson; Participation on Advisory boards from AstraZeneca and Chiesi; all payments to his institution. SOS report leadership roles in the P4O2 consortium (board member) and eVoiceNet EU Cost Action (management committee). SOS reports a pending patent on telemonitoring for respiratory health, published on 12 March 2026. None of the other authors has any conflicts of interest, financial or otherwise, to disclose.

Abstract

Background

Magnetic resonance imaging (MRI) is known to offer the best structural and functional pulmonary assessment and is a promising tool for monitoring and tracking disease progression in prematurity-related lung disease (PRLD).

Objective

We aimed to test the feasibility of capturing anatomical correlates of PRLD with MRI using the bronchopulMonary rottErdam mRi morpholoGy scorE (MERGE-BPD score), and correlating imaging with histological, and functional, lung analysis.

Materials and methods

In this pilot study, 8 sheep from a larger cohort underwent pulmonary MRI at 1 year of age: 4 term-born lambs and 4 preterm-born lambs, of which two were exposed to intra-amniotic lipopolysaccharide (LPS). Besides MRI, lung function was measured using respiratory oscillometry, and histological analysis was performed on post-mortem lung tissue. Statistics were performed using the Kruskal-Wallis test and the Mann-Whitney test, and Z-scores were calculated.

Results

Areas of hyperintensity of lung parenchyma could be identified in all preterm-born animals and in one of the four term-born sheep. MRI changes are associated with histological changes driven by inflammation (− 0.97, 1.24, and 0.48 (overall *p* 0.04)) and mucus plugging (− 0.87, 0.86, and 0.82 (overall *p* 0.07)). Bronchial hyperreactivity was significantly different between the three groups (p 0.05).

Conclusion

We demonstrate that pulmonary MRI complements conventional lung function and histological analysis by detecting subtle abnormalities in prematurity-related lung diseases. It has the potential to become a valuable, safe, and radiation-free tool for predicting lung function trajectories in children and gaining a deeper understanding of pathophysiological mechanisms following preterm birth.

Introduction

Preterm birth increases mortality risks from infancy through adulthood, with respiratory disorders being a major contributor (1). The most well-known prematurity-related respiratory condition is bronchopulmonary dysplasia (BPD); however, children born preterm without BPD are also prone to developing respiratory symptoms later in life. This has led to the broader concept of prematurity-related lung disease (PRLD), a heterogeneous entity with, to date, a poorly defined pathophysiology (2, 3).

Lung function tests are the standard for assessing pulmonary function and are commonly used to detect or screen for PRLDs, but they have limitations. Measuring lung function is particularly challenging in young children, and lung function measurements do not fully capture the anatomical changes associated with PRLD. As a result, knowledge gaps remain about the course and pathogenesis of PRLD, and pulmonary imaging may therefore be helpful in detecting and phenotyping PRLD.

Computed tomography (CT) is currently considered the gold standard for imaging lung structure in children with BPD (4). However, routine use of CT in children is restricted by concerns of radiation exposure. In this context, lung magnetic resonance imaging (MRI) emerges as a promising tool for monitoring and tracking disease progression. MRI is known to offer the best structural and functional assessment, without patient safety concerns, making this technique promising for personalized, longitudinal care in PRLD. Risk scores for infants with severe BPD using lung MRI exist, but these have not yet been applied to the wider PRLD population (5–7). Also, the extent to which changes in MRI correlate with the pathological and functional substrates of PRLD is not well established.

To further explore the correlation between MRI images and the underlying pathology in PRLD, we conducted a pilot study using MRI images from a long-term sheep cohort. These animals were either term-born sheep, preterm-born sheep, or preterm-born sheep exposed to perinatal inflammation. This setup closely mimics pulmonary development and pathophysiological PRLD-like processes observed throughout life in preterm infants. Our primary aim was to test the feasibility of the bronchopulMonary rottErdam mRi morpholoGy scorE (MERGE-BPD score (6)), adapted from the original chest CT score PRAGMA-BPD (4)), for quantifying anatomical changes from lung MRIs. We hypothesized that the MERGE-BPD score could capture anatomical changes in our PRLD animal model, thereby enabling a unique correlation among histological, functional, and pulmonary imaging analyses. This approach would offer a unique opportunity to establish the value of lung MRI in the broader population of (young) infants with PRLD, ultimately advancing understanding of the underlying processes that drive this disease.

Methodology

Animal model

In our translational research laboratory, a long-term Texel sheep study has been conducted, during which a convenience sample of 8 sheep underwent pulmonary MRI. The current study employed an exploratory design; therefore, the sample size was not based on a power calculation. Animal experiments were approved by the Central Authority for Scientific Procedures on Animals and the Animal Welfare Body.

For MRI analysis, we included 4 term-born lambs (~ 150d gestational age (GA)), and 4 preterm lambs (instrumented 121d, betamethasone 131d, cesarean section 132d), of which two were additionally exposed to intra-amniotic lipopolysaccharide (LPS) (125d). Thereafter, preterm animals were mechanically ventilated (MV) for 72 hours as described by Neuen et al. and received standard of care

(8). The term-born lambs were reared by the ewe and weaned at two months. Preterm-born lambs were bottle-fed by animal caretakers. After two months, the reference lambs were housed with age-matched preterm lambs. Lambs were weighed weekly and fed ad libitum.

MRI image acquisition and scoring

At 1 year of age, the animals underwent pulmonary MRI. Before the MRI, the animals were intubated and underwent anesthesia. Animals were sedated with propofol (12 mg/kg/min) and mechanically ventilated by volume guaranteed ventilation (5-6ml/kg/min). Supplemental oxygen was adjusted according to oxygen saturation measurements. As the standard of care, all animals receive 20 ml/kg vascular filling to prevent propofol-induced hypotension.

A chest MRI was performed on a 3-Tesla scanner (Ingenia, Philips Healthcare, Best, the Netherlands) using a 16-channel torso coil. The protocol included a 5mm 3d balanced turbo field echo (BTFE) T2-weighted in coronal and axial plane, 3d Ultrashort echo time (UTE) Proton Density weighted (PD-w) with 1.7 mm isotropic voxels and a spiral acquisition, and 5mm 2d T2-weighted Multivane in axial plane. Respiratory gating with a trigger belt was used to acquire images at the end of expiration during tidal breathing, thereby minimizing motion artifacts. Average scan time was 31 min and 45 seconds.

Eight animals were scored independently by two experienced image analysts. The four 'term-reference sheep' were used as visual references and scored to identify what can be considered normal, particularly with respect to bronchial and vascular tree anatomy and dimensions. Scorers were blinded to the LPS+/- status of the 4 preterm animals. The MERGE-BPD score was used as developed and previously published (6, 9). The MERGE score quantifies pulmonary abnormalities in categories, namely hyper- and hypointensity and bronchopathy, which were calculated as percentages (%) of total lung volume. Hypointense areas include mosaic perfusion, emphysema, trapped air, and bullae. Hyperintense areas include consolidation, atelectasis, and linear/subpleural opacities. Bronchopathy was defined as either bronchiectasis and/or bronchial wall thickening on MRI.

Lung processing and histology

Post-mortem tissue was sampled as described earlier by Neuen et al. (8). Lung sections from the right lower lobe were stained with hematoxylin-eosin, and Carnoy-fixated sections were stained with Alcian Blue-Periodic Acid Schiff. Immunohistochemistry for smooth-muscle cells/myofibroblasts (α-SMA) was described earlier (10). All analyses were performed by two blinded researchers using QuPath (v0.5.0) (11). Bronchioles were defined by the absence of cartilage and submucosal glands, and their counts were quantified per unit of tissue surface area. The thickness of smooth muscles and the thickness of the epithelial layer were measured as tissue area per length of the basal membrane. Mucus-filled bronchioles are defined by containing AB-PAS-positive mucus-producing cells. The percentage of mucus-filled bronchioles or inducible bronchus-associated lymphoid tissue (iBALT) adherent bronchioles was

calculated relative to the total number of bronchioles. The quantitative number of α-SMA in the alveolar compartment was calculated as a percentage of tissue area.

Lung function

At 1 year of age, lung function was assessed by respiratory oscillometry using the Tremoflo c-100 system (Thorasys, Montreal, Canada). Measured parameters included respiratory resistance (R7, R7-20) and reactance (AX). Airway hyperresponsiveness was evaluated using a methacholine provocation test according to the European Respiratory Society guidelines. The provocation dose (PD_{20}) was defined as the dose at which 20% deterioration in lung function (reactance) was achieved.

Statistical analysis

Data are presented as medians (interquartile ranges), with p-values considered statistically significant at < 0.05. p-values were calculated using the Kruskal-Wallis test for 3-group comparison, and the Mann-Whitney test for pairwise comparison. Z-scores were calculated based on eight animals. Graphs and statistical tests were performed using GraphPad Prism version 8.0.2.

This study was reported in accordance with the ARRIVE 2.0 guidelines.

Results

Areas of hyperintensity of lung parenchyma could be identified in all preterm-born animals and in one of the four term-born sheep (Table 1). Figure 1 shows representative free-breathing PD-weighed UTE images. Histological analysis of the lung showed severe damage with signs of tissue remodeling, with fibrosis precursor changes, infiltration, and fluid accumulation in the preterm-born lambs only. No anatomical distortion was seen in the term-born animals. Alternatively, the areas of hyperintensity on MRI could be related to mucus accumulation, which was seen more frequently in histological samples from preterm animals (p 0.04, Table 2).

Although airway changes were seen on histology, MRI-based scoring proved more challenging. Bronchopathy was observed in only a few animals due to high variability in airway diameters and wall thickness, even in the term-born references. These bronchopathy results were not summarized due to the sparsity of data points.

Table 1
GROUPED

Diseased lung	**Term (n = 4)**	**Preterm (n = 2)**	**Preterm + LPS (n = 2)**	**p Value**
	0,00 (0,00–0,00)	**0,12 (0,00–0,29)**	**1,49 (0,97–2,31)**	**0,04 (0,09[1], 0,09[2], 0,33[3])**
Hyperintensity	0,00 (0,00–0,04)	0,33 (0,29–0,37)	2,94 (2,31–3,57)	**0,04** (0,09[1], 0,09[2], 0,33[3])
Bronchopathy	0,00 (0,00–0,00)	0,00 (0,00–0,00)	0,65 (0,32–0,97)	0,22 (1,00[1], 0,29[2], 0,62[3])
Normal lung	100 (99,96–100)	99,67 (99,63–99,71)	96,41 (95,46–97,36)	**0,04** (0,09[1], 0,09[2], 0,33[3])

Note: Quantitative MRI results according to the MERGE scoring. Data are presented as % of the total lung volume.[1]represents term vs. preterm.[2]represents term vs. preterm + LPS.[3]represents preterm vs. preterm + LPS.

Table 2
– GROUPED

Nr. bronchioles	**Term (n = 4)**	**Preterm (n = 2)**	**Preterm + LPS (n = 2)**	**p Value**
	0,64 (-0,08 – 1,30)	**-0,28 (-0,40 - -0,15)**	**-0,90 (-0,96 - -0,83)**	**0,11 (0,53[1], 0,13[2]. 0.33[3])**
Epithelial heightening	-0,36 (-0,54 - -0,30)	-0,32 (-0,47 - -0,16)	1,28 (0,77–1,79)	0,13 (0,80[1], 0,13[2], 0,33[3])
Smooth muscle thickness	-0,74 (-1,01 - -0,14)	0,05 (-0,10– 0,20)	0,78 (0,35–1,20)	0,29 (0,53[1], 0,27[2], 0,67[3])
Mucus	-0,97 (-0,97 – – 0,86)	1,24 (1,13– 1,35)	0,48 (0,28–0,66)	**0,04** (0,09[1], 0,09[2], 0,33[3])
iBALT	-0,87 (– 1,35 – -0,37)	0,86 (0,85– 0,88)	0,82 (0,66–0,98)	0,07 (0,13[1], 0,13[2], 1,00[3])
Edema	-0,60 (-0,72 - -0,36)	-0,42 (-0,51 - -0,33)	1,39 (0,95–1,82)	0,12 (0,81[1], 0,10[2], 0,33[3])
a-SMA myofibroblast	-0,60 (-1,01 - -0,16)	0,27 (-0,12– 0,66)	0,87 (0,64–1,11)	0,29 (0,53[1], 0,27[2], 0,67[3])

Note: Histological data presented in z-scores. [1] represents term vs. preterm. [2] represents term vs. preterm + LPS. [3] represents preterm vs. preterm + LPS.

Lung function is shown in Table 3. Bronchial hyperreactivity was significantly different between the three groups (p 0.05). However, significance was lost in the post hoc groupwise comparison. Preterm animals had the lowest lung function scores, although these differences were not statistically significant in the group comparison in our small sample (Table 3).

Table 3
– GROUPED – LUNG FUNCTION

R7	Term (n = 4)	Preterm (n = 2)	Preterm + LPS (n = 2)	p Value
	0,75 (0,32–1,07)	**-0,60 (-0,82 – -0,37)**	**-0,67 (-1,06 – -0,29)**	**0,22 (0,27[1], 0,27[2], 1,00[3])**
R7-20	0,23 (-0,55–0,86)	0,60 (0,23–0,96)	-0,74 (-0,96 – -0,52)	0,26 (0,53[1], 0,53[2], 0,33[3])
AX	0,91 (0,67–1,06)	-0,67 (-0,91 – -0,43)	-0,98 (-1,15 – -0,81)	0,06 (0,13[1], 0,13[2], 0,67[3])
PD_{20}	0,48 (-0,11–1,26)	-0,88 (-0,91 – -0,85)	-0,46 (-0,56 – -0,36)	**0,05** (0,13[1], 0,13[2], 0,33[3])

Note: Lung function data presented in z-scores per group. [1] represents term vs. preterm. [2] represents term vs. preterm + LPS. [3] represents preterm vs. preterm + LPS.

Discussion

In the current exploratory study using an animal model that mimics PRLD, we showed the possibilities of pulmonary MRI for assessing structural lung abnormalities in PRLD. We demonstrated that MRI changes are associated with histological changes driven by inflammation and mucus plugging in individual animals. Importantly, individual preterm animals also showed increased airway hyperreactivity. These changes seen on MRI cover part of the PRLD spectrum, and thus offer the opportunity to further investigate this subtype non-invasively (12).

MRI showed increased hyperintensity in all preterm animals, whereas this finding was observed in only one term-born animal. These changes may reflect atelectasis caused by mucus plugging or inflammation-induced consolidation, as histological analysis demonstrated comparable mucus formation. Further differentiation was not possible because of the limited spatial resolution of MRI. Mucus clearance may be underestimated in descriptions of the PRLD phenotype, as it has been less extensively investigated than other pathological features. Importantly, previous studies have shown that such abnormalities are associated with long-term impairment of lung function, and that additional environmental triggers later in life (e.g., cigarette smoke or viral infections) may further exacerbate functional decline (13).

Pulmonary abnormalities persisted after 1-year follow-up in our sheep model, corresponding to young adulthood in humans. Therefore, pulmonary MRI may serve as an additional valuable tool for discriminating between groups compared with lung function alone during longitudinal follow-up. Observations of structural changes in sheep at 1 year of age indicate that perinatal insults during critical early development can lead to lung structural and functional changes that persist into adulthood. Moreover, our findings extend the results of a previous clinical study showing lung damage on MRI in

preterm-born children at 6 years of age (14). In our study, these imaging-based adverse outcomes were associated with impairments in lung function. This tentatively connects the early anatomical changes with studies reporting obstructive lung function in former preterm-born individuals, including persistent respiratory symptoms into adulthood, even among moderate-to-late preterm groups (15–17).

From a preclinical perspective, pulmonary MRI strengthens our research model by providing a unique correlation between imaging, histology, and lung function. Although the prevalence of detectable abnormalities was low, this aligns with reports in humans, where hyperattenuation of lung tissue on CT occurs at similar rates (18). Moreover, literature indicates that other MRI sequences can identify hypo- and hyperintense abnormalities, bronchopathy, and architectural distortion, which are consistent with CT-based findings (6). The lower spatial resolution of MRI compared to CT is acknowledged, but MRI offers clear advantages over CT. Not only can full inspiration and expiration scans be acquired, but MRI allows a comprehensive evaluation of lung structure as well as functional alterations in ventilation. Recent studies support this by showing that MRI can detect progressive parenchymal changes while also providing quantitative insights into ventilation distribution and pulmonary vascular development in BPD (19–21).

Developing novel imaging methods is important in children with PRLD. It may identify children who are at risk of developing pulmonary complications later in life. Unlike traditional lung function tests, MRI can reveal subtle injuries with prognostic value even in preterm-born children without BPD who show normal spirometry results (6). Also, long-term follow-up would be possible through sequential MRI, given that some children develop significant morbidity despite minimal initial impairment (22). We showed that MRI use could be extended to moderate-to-late preterm infants, for whom adequate guidelines, screening, and monitoring are currently lacking. Recent advances in ultrafast MRI techniques and free-breathing sequences have made pulmonary MRI more feasible for young children who are unable to hold their breath (23). Beyond phenotyping neonatal lung diseases, MRI can support precision medicine approaches, tailor interventions (e.g., steroid responsiveness), and monitor therapy response over time, all without radiation-related long-term risks (5).

Several limitations need to be considered. This includes the small size of our population and the lack of longitudinal data. There were also technical limitations, such as inconsistent detection of hypointensity and bronchopathy with our MRI sequence, and wide variability in airway diameter and wall thickness among control animals, which reduced the sensitivity of our findings. Lastly, maximal inspiration and expiration scans could not be obtained with this mechanical ventilator and MRI setup in this pilot.

Conclusion

Our study in an ovine model demonstrates that pulmonary MRI complements conventional lung function and histological analysis by detecting subtle abnormalities in prematurity-related lung diseases. While these are pilot data, they provide evidence for the potential of lung MRI as a tool for monitoring lung

damage in children after preterm birth and for providing a deeper understanding of the underlying pathophysiological mechanisms.

Declarations

Competing Interests

SOS reports grants from Roche, Dutch Research Council (NWO) and Lung Foundation Netherlands (Longfonds); Honoraria for lectures from AstraZeneca,Chiesi, and Johnson & Johnson; Participation on Advisory boards from AstraZeneca and Chiesi; all payments to his institution. SOS report leadership roles in the P4O2 consortium (board member) and eVoiceNet EU Cost Action (management committee). SOS reports a pending patent on telemonitoring for respiratory health, published on 12 March 2026. None of the other authors has any conflicts of interest, financial or otherwise, to disclose.

Author Contribution

Conceived and designed research: TB, TGAMW, MCH, and SOS. Performed experiments: TB. Analyzed data: TB, DC, PC, and MB. Interpreted results of experiments: TB, SOS, DC, PC, and MCH. Prepared figures: TB. Drafted manuscript: TB and SOS. Edited and revised manuscript: TB, MCH, RGCS, DC, PC, LZ, TGAMW, and SOS. Approved final version of manuscript: TB, SMLN, MCH, RGCS, DC, PC, MB, LZ, DRMGO, NLR, TGAMW, and SOS.

Acknowledgement

We gratefully thank the radiology department from the MosaKids Children’s Hospital, Maastricht University Medical Centre+, and especially Maikel Junghans and Etienne Lemaire for excellent experimental support.

Data Availability

The datasets generated and/or analyzed during the current study are available from the corresponding author upon request.

References

1. Ahmed AM, Grandi SM, Pullenayegum E, McDonald SD, Beltempo M, Premji SS et al (2024) Short-Term and Long-Term Mortality Risk After Preterm Birth. JAMA Netw Open 7(11):e2445871
2. Thébaud B, Goss KN, Laughon M, Whitsett JA, Abman SH, Steinhorn RH et al (2019) Bronchopulmonary dysplasia. Nat Reviews Disease Primers. ;5(1)

3. Bancalari E, Jain D (2019) Bronchopulmonary Dysplasia: 50 Years after the Original Description. Neonatology 115(4):384–391
4. Van Mastrigt E, Logie K, Ciet P, Reiss IKM, Duijts L, Pijnenburg MW et al (2016) Lung CT imaging in patients with bronchopulmonary dysplasia: A systematic review. Pediatr Pulmonol 51(9):975–986
5. Vanhaverbeke K, Van Eyck A, Van Hoorenbeeck K, De Winter B, Snoeckx A, Mulder T et al (2020) Lung imaging in bronchopulmonary dysplasia: a systematic review. Respir Med 171:106101
6. Elders BBLJ, Tiddens HAWM, Pijnenburg MWH, Reiss IKM, Wielopolski PA, Ciet P (2022) Lung structure and function on MRI in preterm born school children with and without BPD: A feasibility study. Pediatr Pulmonol 57(12):2981–2991
7. Förster K, Marchi H, Stöcklein S, Dietrich O, Ehrhardt H, Wielpütz MO et al (2023) Magnetic resonance imaging-based scoring of the diseased lung in the preterm infant with bronchopulmonary dysplasia: UNiforme Scoring of the disEAsed Lung in BPD (UNSEAL BPD). Am J Physiology-Lung Cell Mol Physiol 324(2):L114–L22
8. Neuen SML, Ophelders DRMG, Widowski H, Hütten MC, Brokken T, Van Gorp C et al (2024) Multipotent adult progenitor cells prevent functional impairment and improve development in inflammation driven detriment of preterm ovine lungs. Regenerative Therapy 27:207–217
9. Fontijn S, Balink SJA, Bonte M, Andrinopoulou ER, Duijts L, Kroon AA et al (2023) Chest computed tomography in severe bronchopulmonary dysplasia: Comparing quantitative scoring methods. Eur J Radiol 169:111168
10. Hoogenboom LA, Lely AT, Kemp MW, Saito M, Jobe AH, Wolfs TGAM et al (2022) Chorioamnionitis Causes Kidney Inflammation, Podocyte Damage, and Pro-fibrotic Changes in Fetal Lambs. Front Pead. ;10
11. Bankhead P, Loughrey MB, Fernández JA, Dombrowski Y, McArt DG, Dunne PD et al (2017) QuPath: Open source software for digital pathology image analysis. Sci Rep. ;7(1)
12. Pierro M, Van Mechelen K, Van Westering-Kroon E, Villamor-Martínez E, Villamor E (2022) Endotypes of Prematurity and Phenotypes of Bronchopulmonary Dysplasia: Toward Personalized Neonatology. J Personalized Med 12(5):687
13. Collaco JM, McGrath-Morrow SA (2021) Bronchopulmonary dysplasia as a determinant of respiratory outcomes in adult life. Pediatr Pulmonol 56(11):3464–3471
14. Förster K, Strobl K, Kindt A, Häfner F, Schubert B, Heinen F et al (2025) Lung MRI scoring reveals persistence of emphysema-like changes in lungs of infants born preterm at (pre)school age. ERJ Open Res 11(5):01183–2024
15. Kotecha SJ, Dunstan FD, Kotecha S (2012) Long term respiratory outcomes of late preterm-born infants. Seminars Fetal Neonatal Med 17(2):77–81
16. Vollsæter M, Røksund OD, Eide GE, Markestad T, Halvorsen T (2013) Lung function after preterm birth: development from mid-childhood to adulthood. Thorax 68(8):767–776
17. Tsang KD, Tramper-Stranders GA, Been JV, Hoffmann-Haringsma AK, Reiss IK, Pijnenburg MWH et al (2025) Moderate-to-late prematurity: understanding respiratory consequences and modifiable risk

factors. Eur Respiratory Rev 34(176):240267

18. Van Mastrigt E, Kakar E, Ciet P, Den Dekker HT, Joosten KF, Kalkman P et al (2017) Structural and functional ventilatory impairment in infants with severe bronchopulmonary dysplasia. Pediatr Pulmonol 52(8):1029–1037
19. Bdaiwi AS, Willmering MM, Woods JC, Walkup LL, Cleveland ZI (2025) Quantifying Spatial Distribution of Ventilation Defects in Multiple Pulmonary Diseases With Hyperpolarized. J Magn Reson Imaging 61(4):1860–1873< scp > < sup > 129Xenon MRI
20. Munidasa S, Higano NS, Willmering MM, Bdaiwi AS, Cordon XH, Elias DB et al (2025) Serial MRI Measures Short-Term Parenchymal Changes in Neonatal Bronchopulmonary Dysplasia. Chest
21. Mukthapuram S, Donaher A, Higano NS, Rowe JA, Tkach JA, Woods JC et al (2024) Magnetic Resonance Imaging Assessment of Pulmonary Vascularity in Preterm Infants with Bronchopulmonary Dysplasia. Neonatology. :1–8
22. Simpson SJ, Turkovic L, Wilson AC, Verheggen M, Logie KM, Pillow JJ et al (2018) Lung function trajectories throughout childhood in survivors of very preterm birth: a longitudinal cohort study. Lancet Child Adolesc Health 2(5):350–359
23. Higano NS, Bates AJ, Gunatilaka CC, Hysinger EB, Critser PJ, Hirsch R et al (2022) Bronchopulmonary dysplasia from chest radiographs to magnetic resonance imaging and computed tomography: adding value. Pediatr Radiol 52(4):643–660

Figures

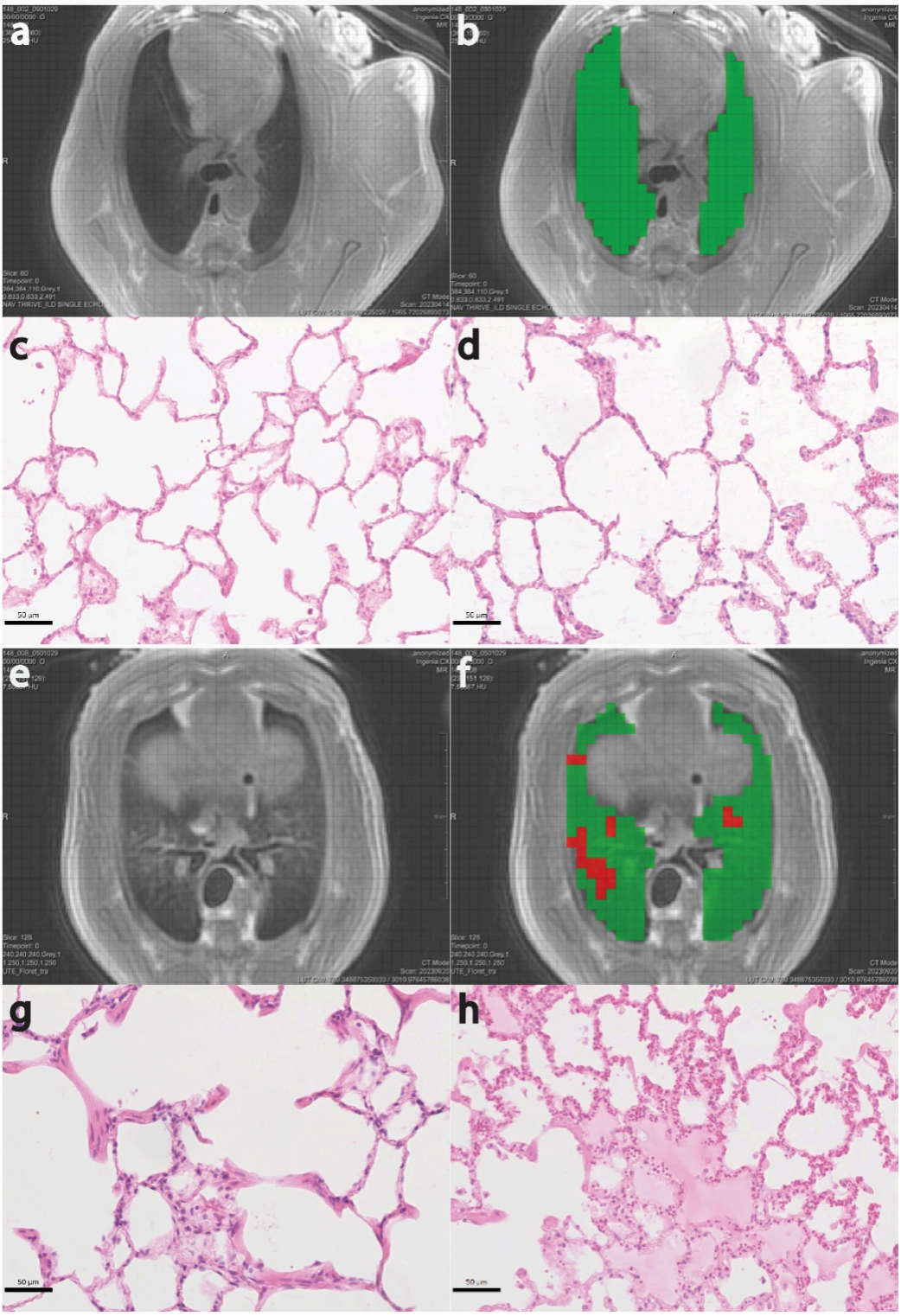


Figure 1

Representative images from pulmonary MRI in sheep, free-breathing PD-weighed UTE sequence. a and b show a term-reference animal, normal sheep anatomy, without signs of hyperintensity of lung tissue. c and d show representative histology images of a term-reference animal. e and f show preterm + LPS with more hyperintense areas, and g and h show representative histological images of a preterm + LPS, with h showing mucus-filled alveoli.